Supporting Information for

Shallow Slow Earthquake Episodes Near the Trench Axis Off Costa Rica

Satoru Baba[1], Kazushige Obara[1], Shunsuke Takemura[1], Akiko Takeo[1], and Geoffrey A. Abers[2]

1. Earthquake Research Institute, The University of Tokyo
2. Department of Earth and Atmospheric Sciences, Cornell University

Contents of this file

Figures S1 to S11
Table S1

## Additional Supporting Information (Files uploaded separately)

Data Set S1
Data Set S2

Introduction

This supporting information file includes eleven figures and one table. Figure S1 shows synthetic and observed waveforms in 0.02–0.05 Hz and 0.02–0.06 Hz. Figure S2 represents the comparison of distributions of epicenters and cross-correlation coefficient distributions when using only vertical component seismograms and both vertical and horizontal component seismograms. Figure S3 illustrates the cross-section of the structure used in the simulation of this study. Figure S4 shows the differences in waveforms for different focal mechanism and depth cases. The examples of waveforms of a very low frequency earthquake and a non-VLFE signal are illustrated in Figure S5. Figure S6 illustrates the distributions of CCs and moment rates when origin time and source duration changed. Figure S7 represents the CC distributions between synthetic and observed waveforms of regular earthquakes in the updip and downdip events. Figure S8 demonstrates examples of waveforms when VLFEs and tremors occur simultaneously. Figure S9 shows observed and simulated waveforms of a tremor which corresponds to a VLFE in the frequency range of 2–8 Hz. Figure S10 presents the distribution of earthquakes used in the estimation of the quality factor and site amplification factors. Figure S11 shows the distribution of CCs between envelopes of station pairs. Table S1 presents the physical parameters of each layer in the velocity structure model used for computing template waveforms.

Additional Supporting Information includes the detected VLFE (Data Set S1) and tremor catalog (Data Set S2).

(a) Event A, CC=0.45
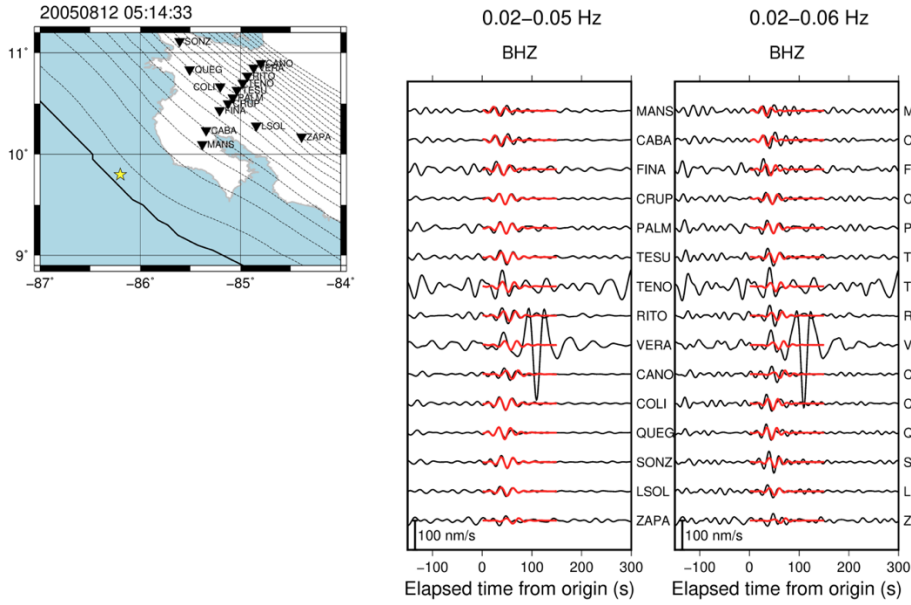
(b) Event B, CC=0.43
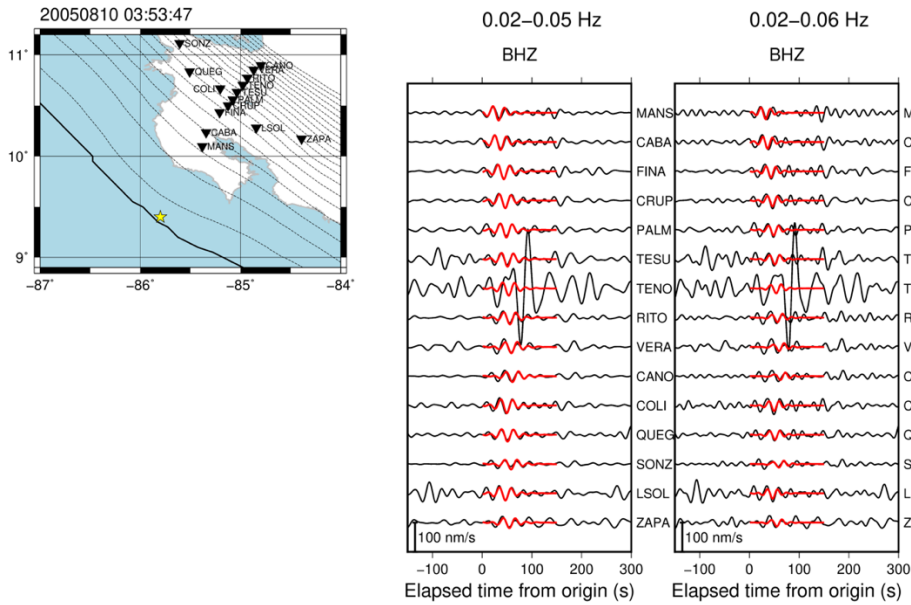
Figure S1. Examples of synthetic (red) and observed (black) waveforms in 0.02–0.05 Hz and 0.02–0.06 Hz. In the map, inverted triangles show locations of stations and the star shows the epicenter located by matched-filter analysis in the frequency range of 0.02–0.05.

(a)

2004/09/18 03:03:43
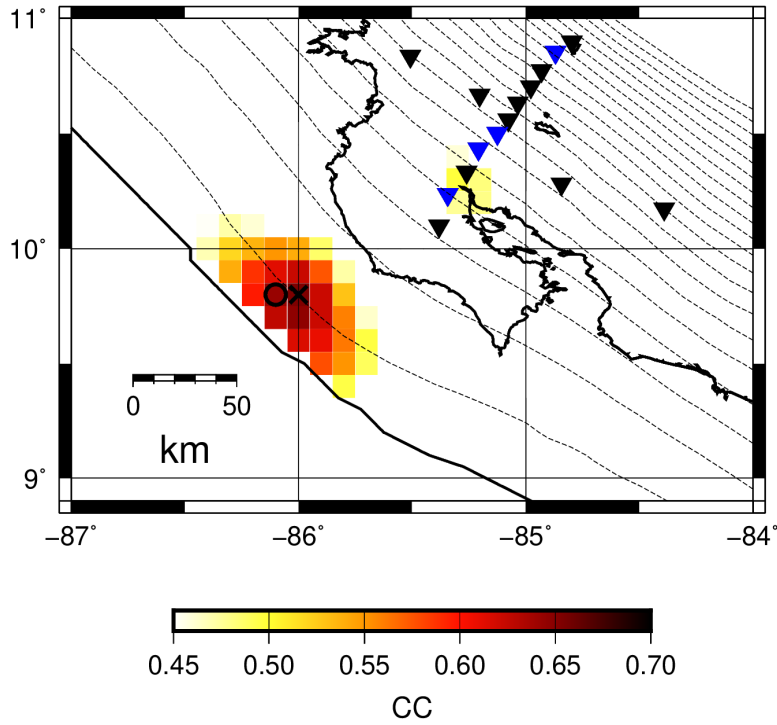

2004/09/18 03:03:43

(b)
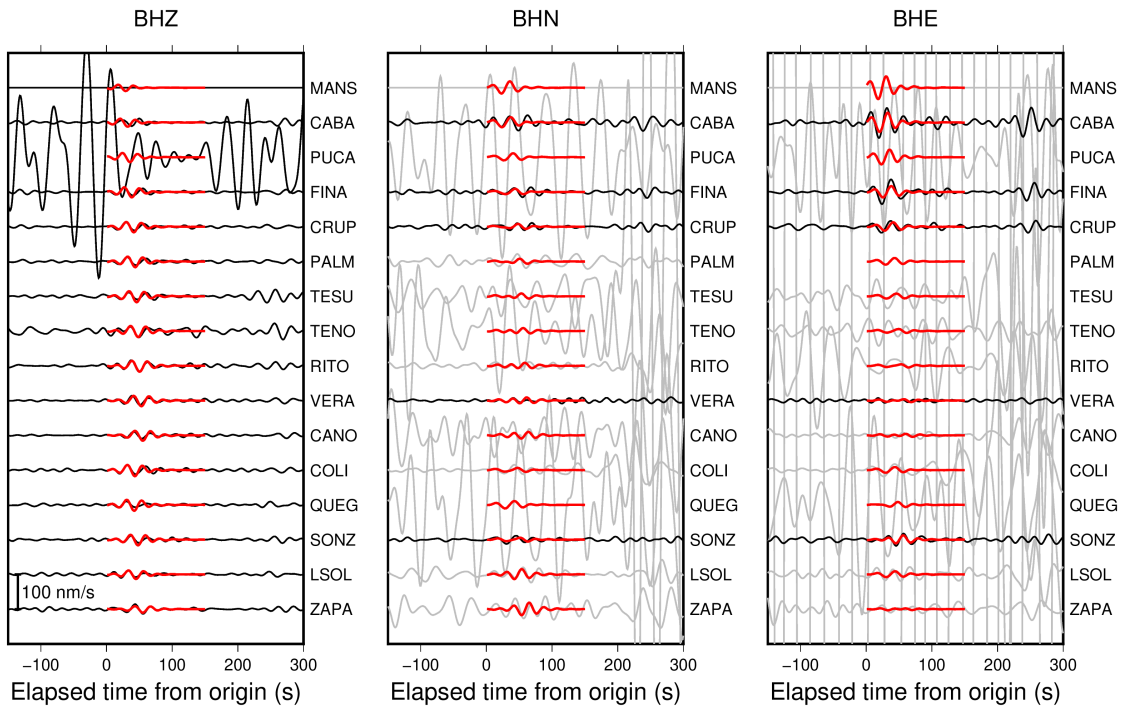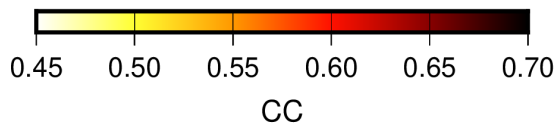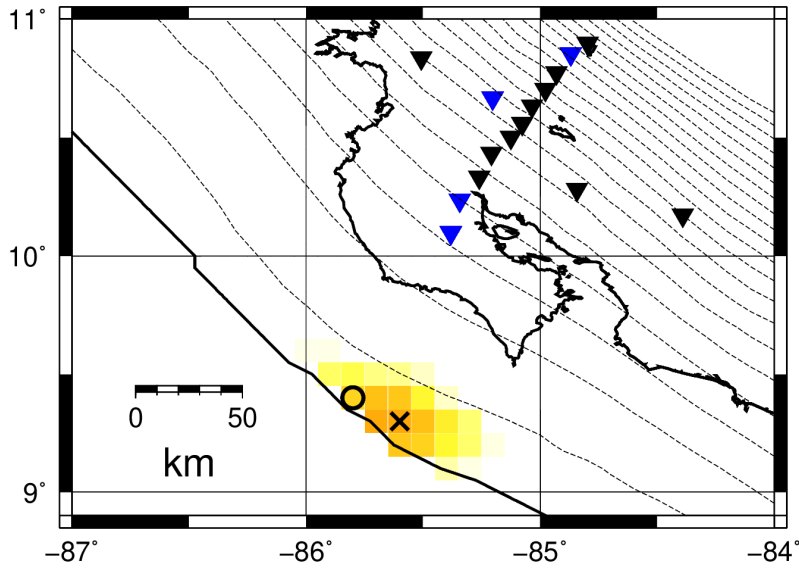
2005/08/10 02:59:06
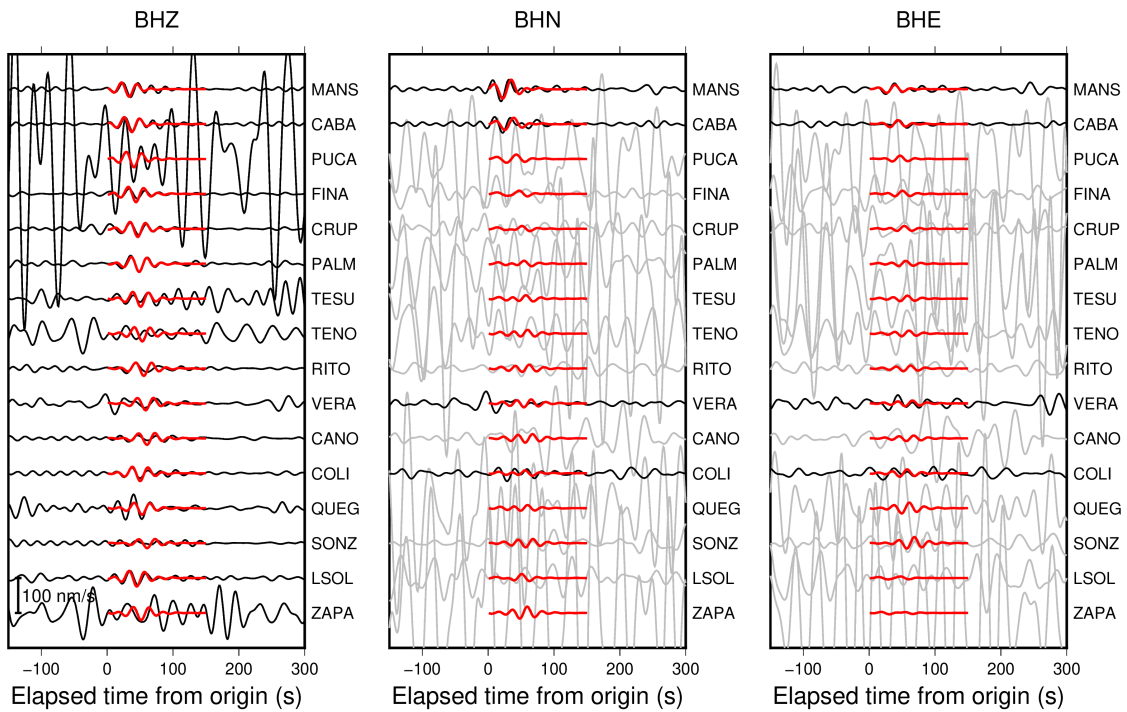
(c)

2005/08/10 03:53:47
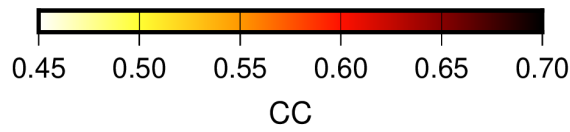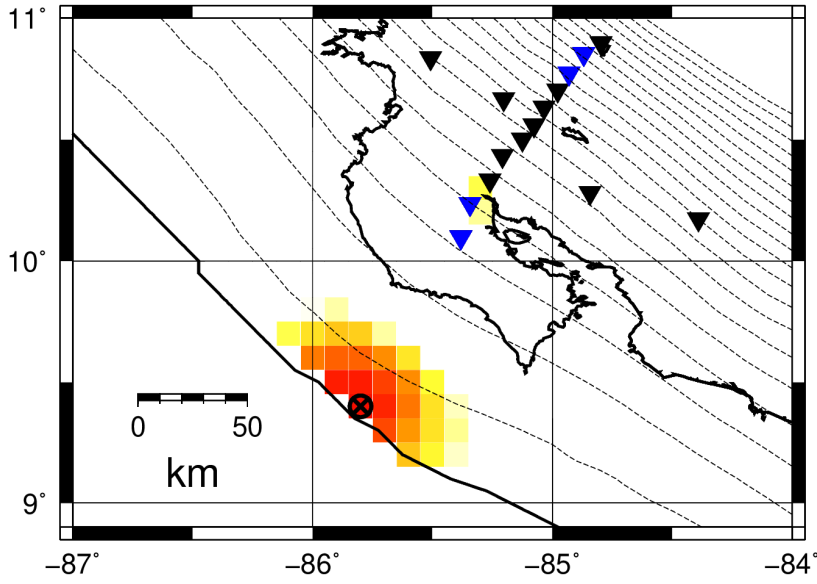

2005/08/10 03:53:47
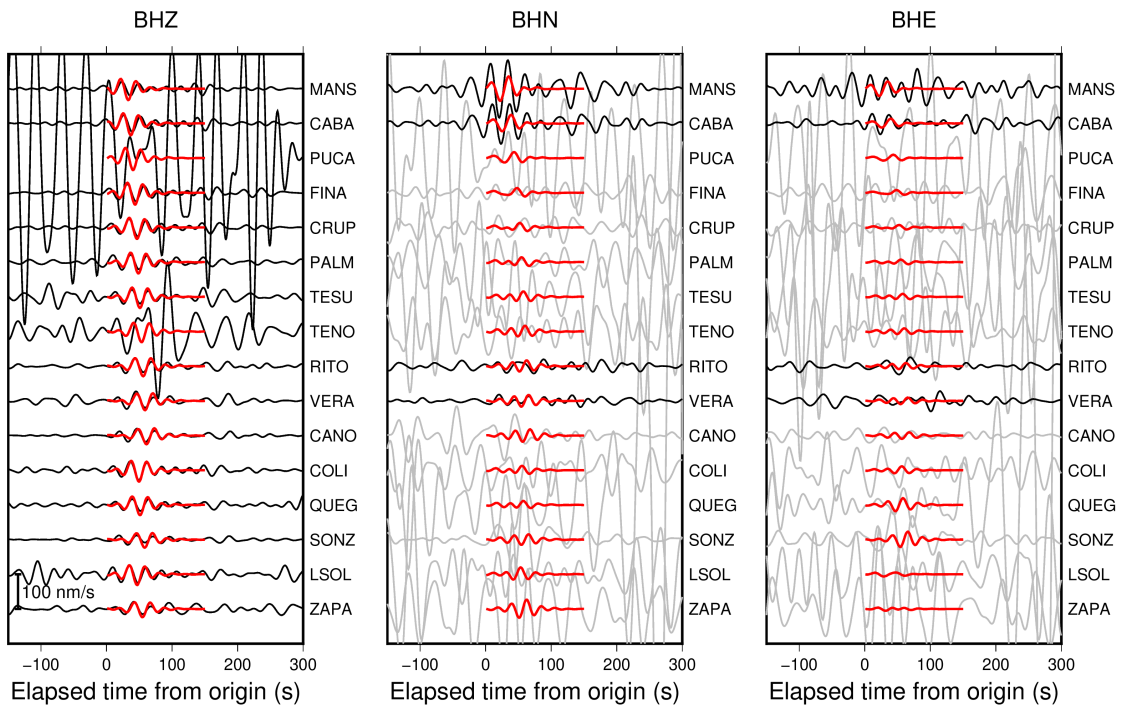
(d)

2005/08/12 05:14:33
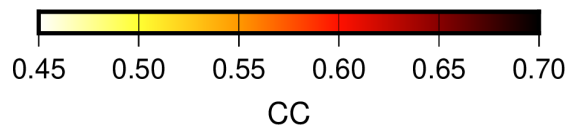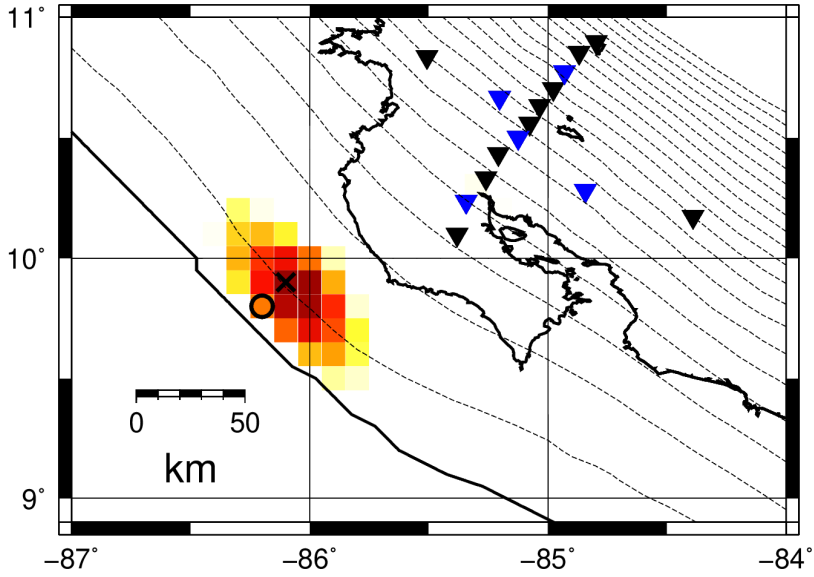
2005/08/12 05:14:33

(e)
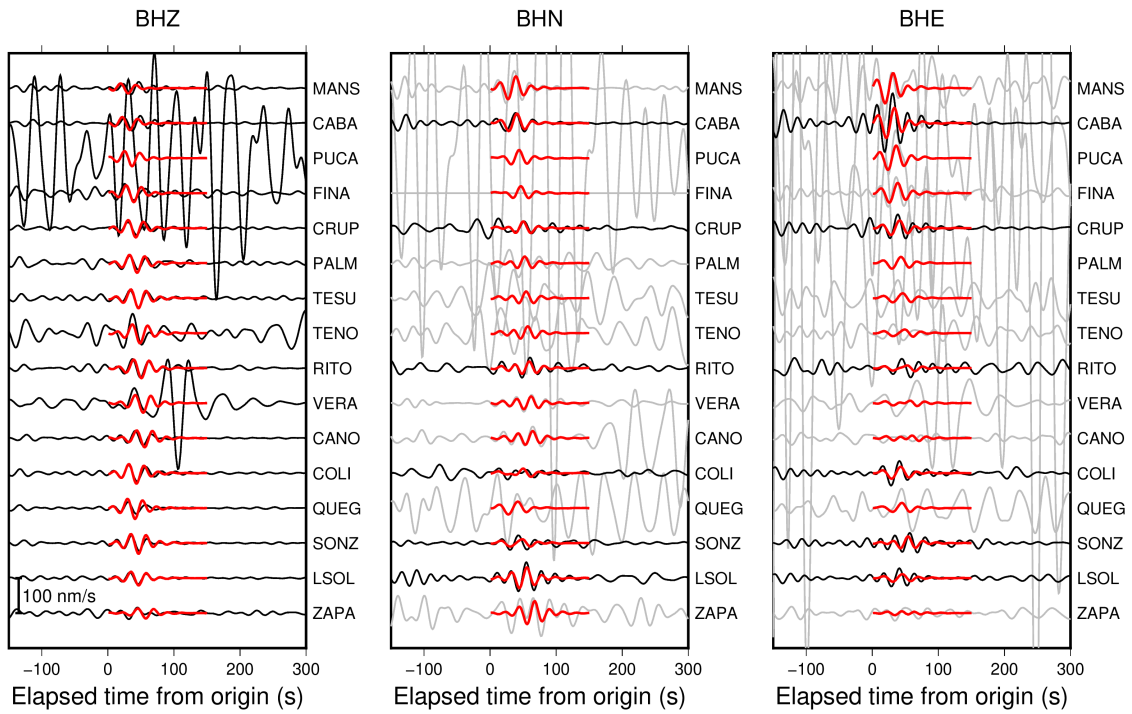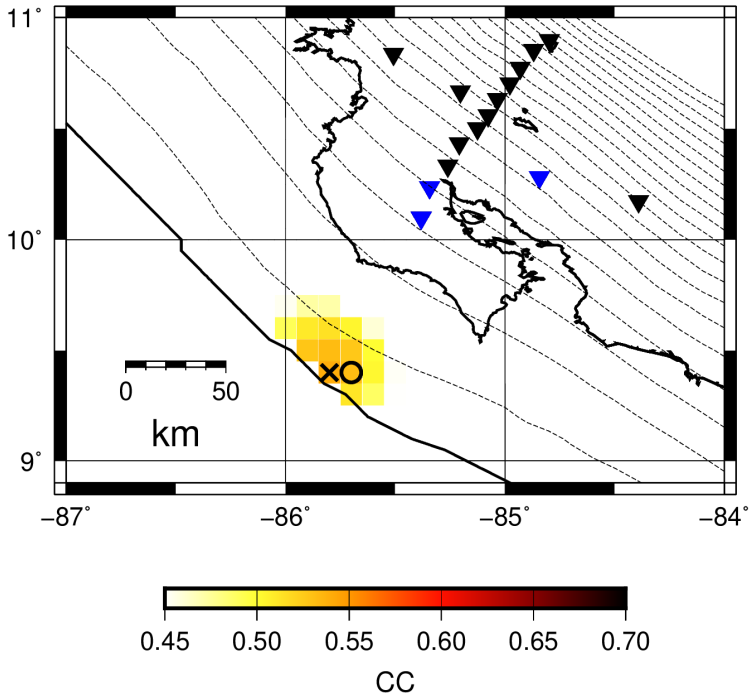
2005/08/18 01:36:28
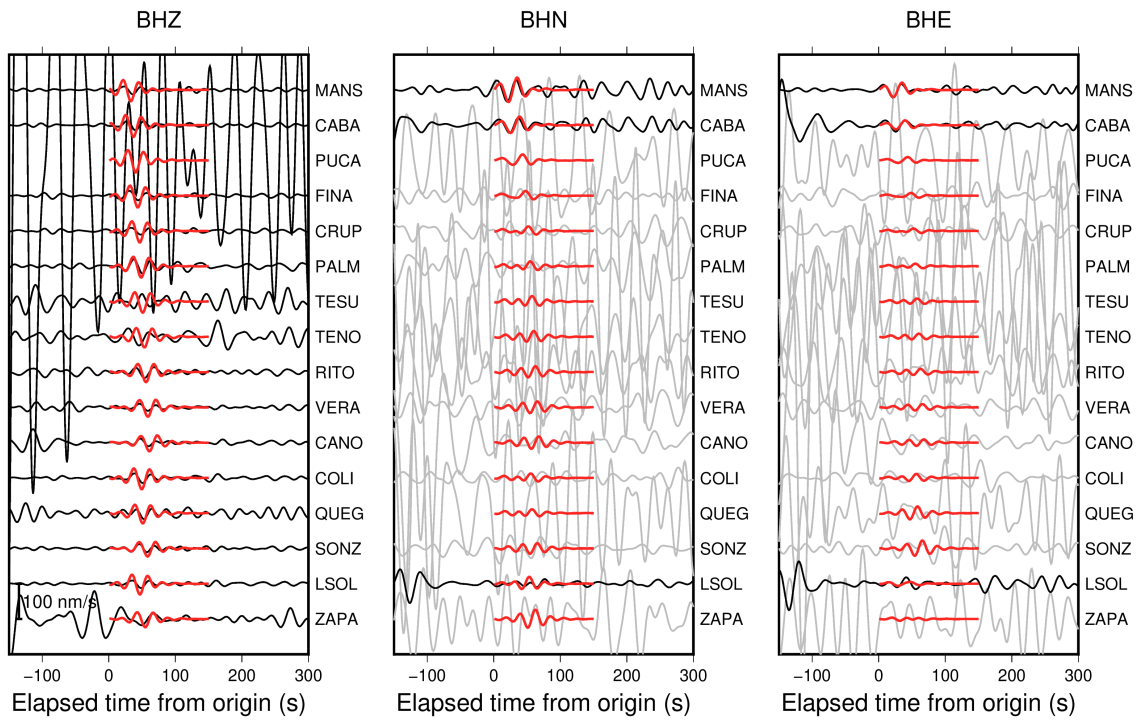
Figure S2. Comparison of epicenters and cross-correlation coefficient (CC) distributions when using three components. Color scales in the maps show CC distributions when three components are used. For horizontal component seismograms, we only used waveforms with lower noise levels (black lines) and did not use waveforms with high noise levels (gray lines). Waveforms are band-pass filtered in the frequency range of 0.02–0.05 Hz. Circles and cross marks in the maps are epicenters when using only vertical component seismograms and both vertical and horizontal component seismograms, respectively. Blue and black inverted triangles in the maps are stations whose three components and only the vertical component seismograms are used for locating very low frequency earthquakes (VLFEs), respectively. Black line and dashed contours in maps are the same as in Figure 1.
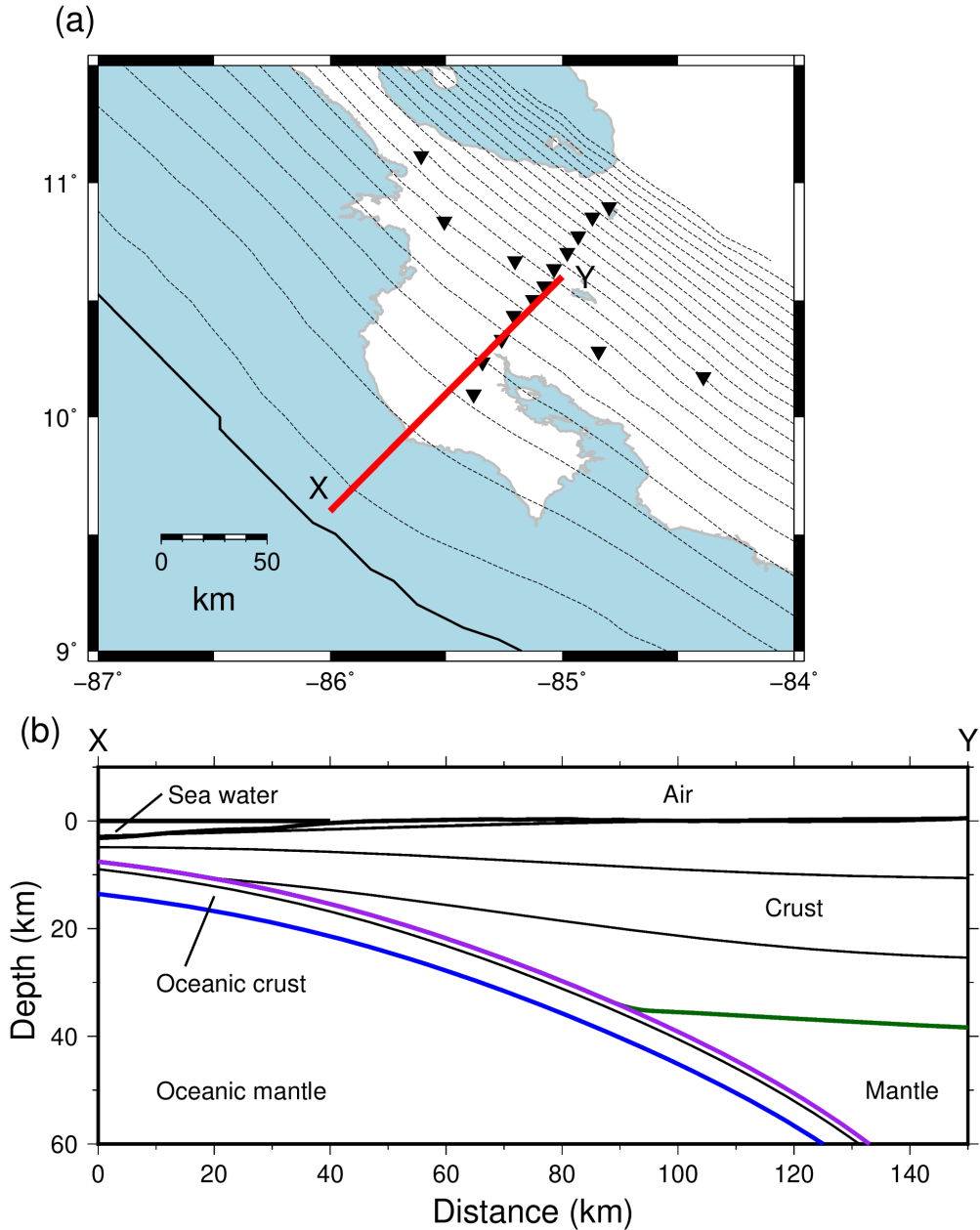
Figure S3. (a) Profile through the model shown in Figure S3b. Dotted lines, black line, and inverted stations are the same as Figure 1. (b) Cross-section of the profile shown in Figure S3a. Dark green, purple, and blue lines indicate the continental Moho, the upper surface of the subducting plate, and the oceanic Moho, respectively. Physical parameters of each layer are listed in Table S1.

(a)
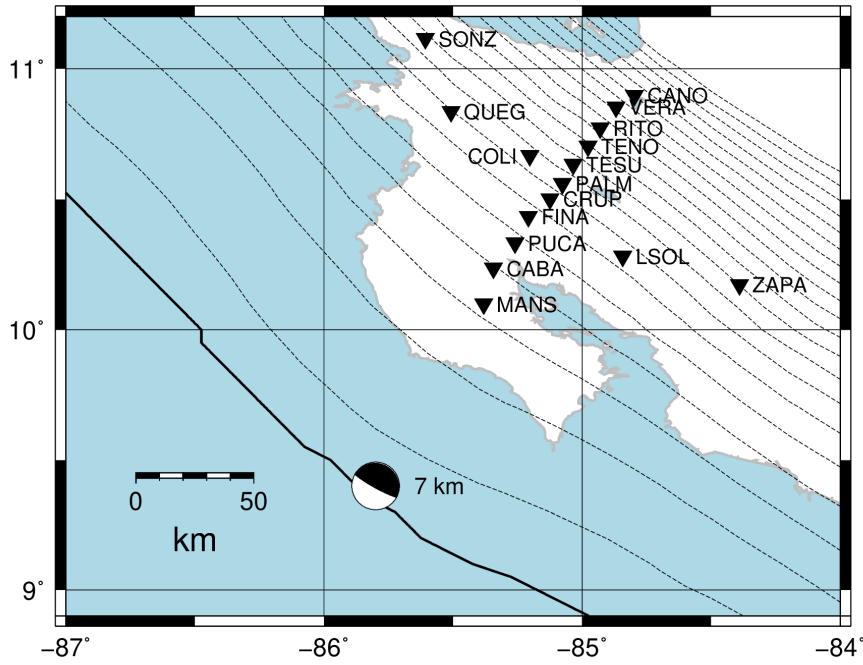
(b) Case A: depth 12 km

(c) Case B: dip 40º

cc 0.83

MANS BHZ
CABA BHZ
PUCA BHZ
FINA BHZ
CRUP BHZ
PALM BHZ
TESU BHZ
TENO BHZ
RITO BHZ
VERA BHZ
CANO BHZ
COLI BHZ
QUEG BHZ
SONZ BHZ
LSOL BHZ
ZAPA BHZ

100 nm/s

Elapsed time from origin (s)

(d) Case C: strike 270º

cc 1.00

MANS BHZ
CABA BHZ
PUCA BHZ
FINA BHZ
CRUP BHZ
PALM BHZ
TESU BHZ
TENO BHZ
RITO BHZ
VERA BHZ
CANO BHZ
COLI BHZ
QUEG BHZ
SONZ BHZ
LSOL BHZ
ZAPA BHZ

100 nm/s

Elapsed time from origin (s)

11
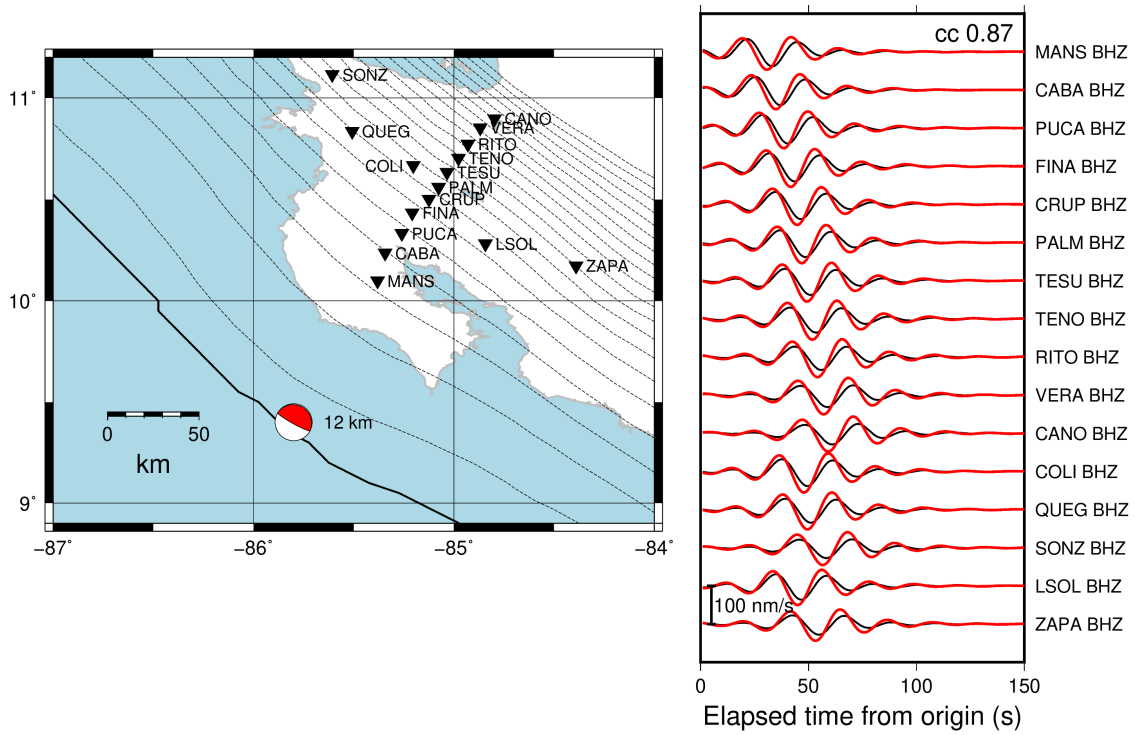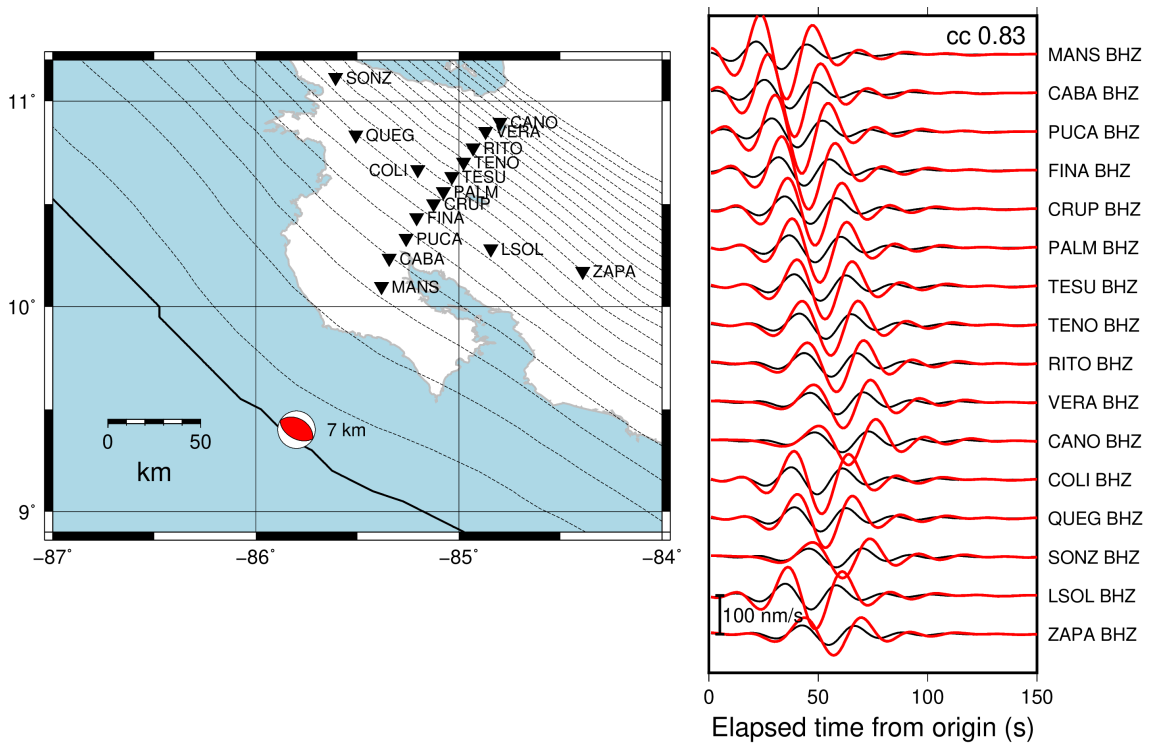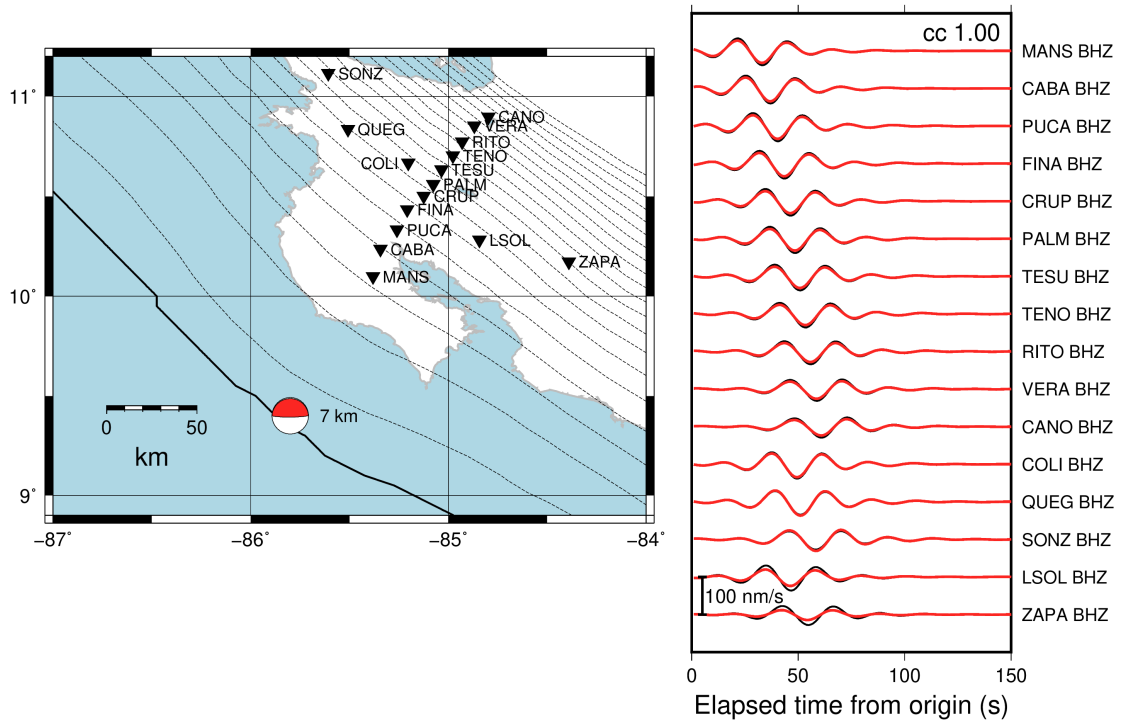
(e) Case D: strike slip
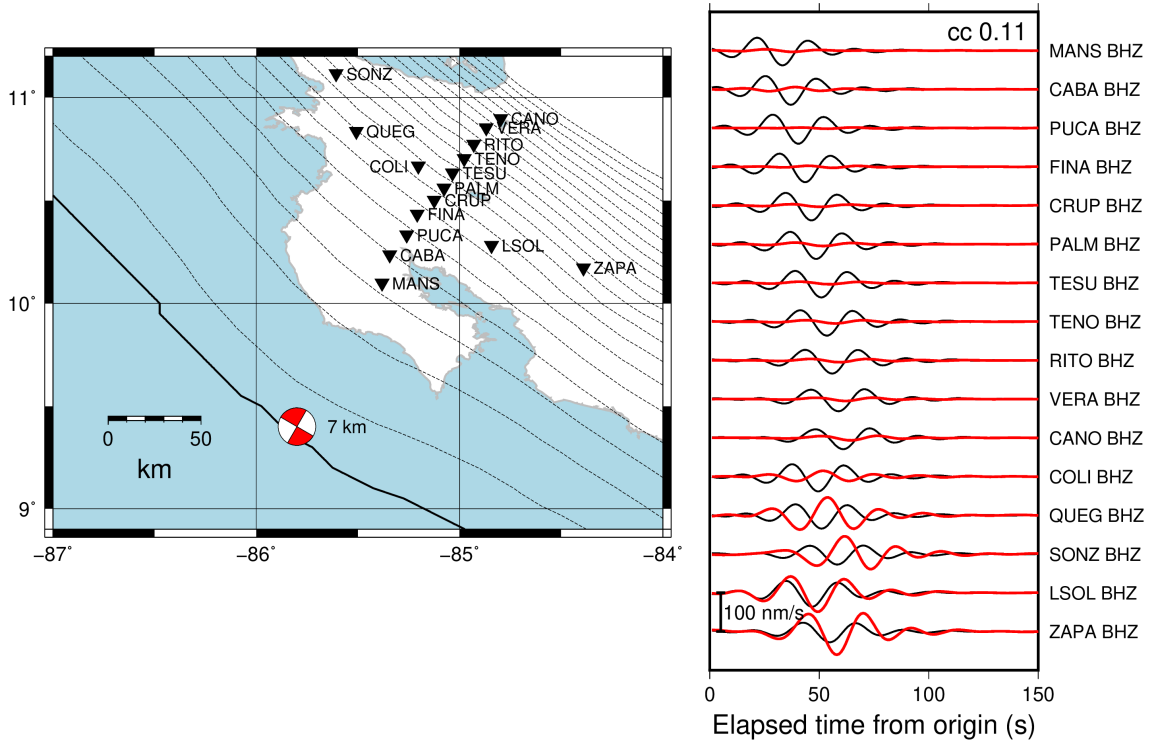
Figure S4. Comparison of waveforms in the frequency range of 0.02–0.05 Hz for different focal mechanism sources. (a) Focal mechanism and depth which are consistent with the geometry of the plate boundary; thrust type with a depth of 7 km, a strike of 299º, and a dip of 6º. (b) Case A: a focal mechanism whose depth is 5 km deeper than the plate boundary. (c) Case B: a focal mechanism whose sip is higher angle than the geometry of the plate boundary. (d) Case C: a focal mechanism whose strike changes in 30º from the geometry of the plate boundary. (e) Case D: a focal mechanism with a strike slip. Black and red lines are waveforms of focal mechanisms which is consistent with the geometry of the plate boundary (beachball is shown in Figure S4a) and those of Cases A-D (beachballs are shown in Figures S4b-S4e), respectively. CCs between black and red waveforms are shown above the waveforms. Inverted triangles, black line, and dashed contours in maps are the same as in Figure 1.

12
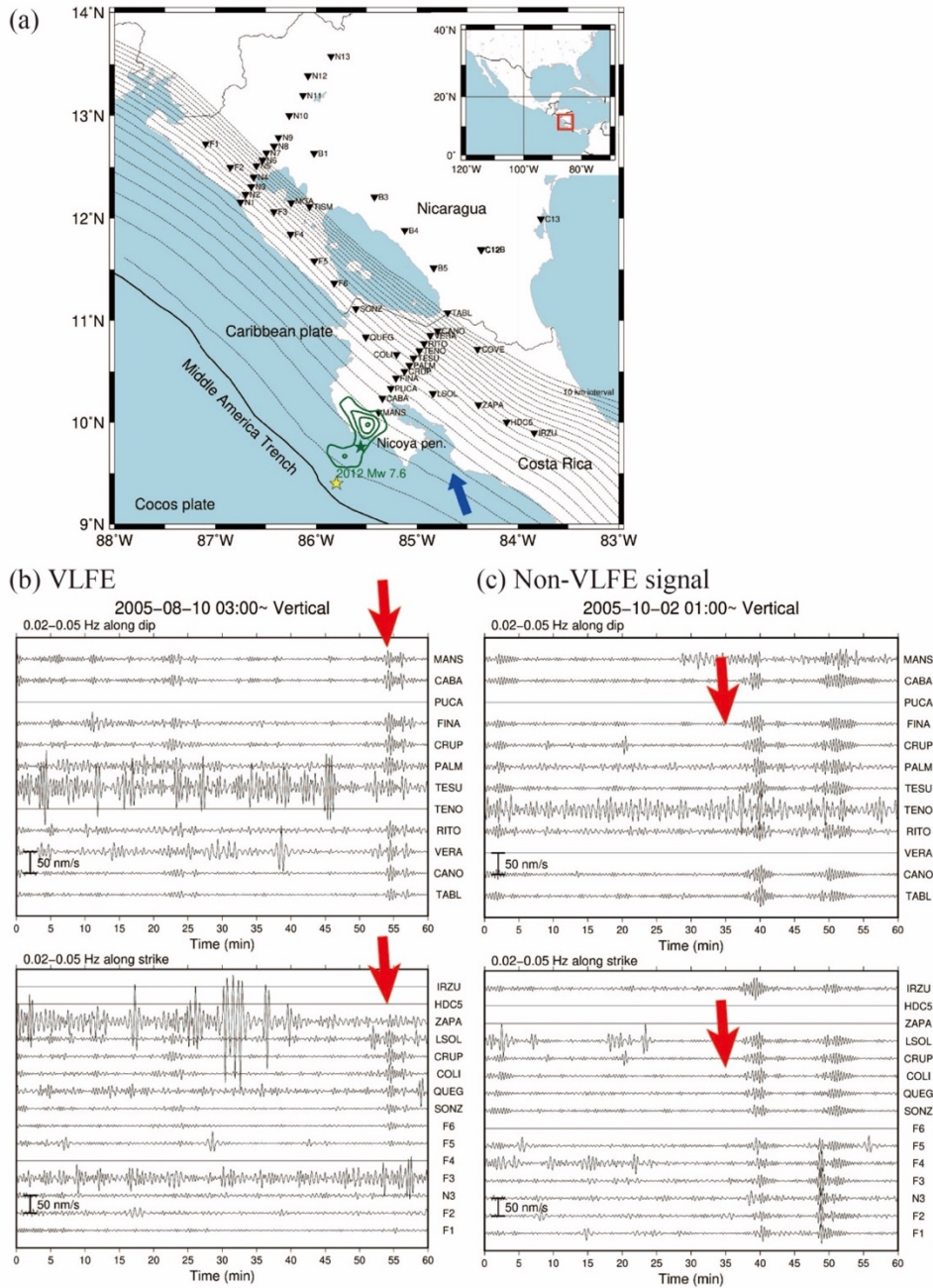
**Figure S5.** (a) Map of stations of TUCAN network in Costa Rica and Nicaragua. Inverted triangles, black line, and dashed contours in maps are the same as in Figure 1. (b) An example of waveforms of a VLFE in the frequency range of 0.02–0.05 Hz for an event with a time of origin 03:53:47 (UTC), August 10, 2005. The epiceneter of this VLFE is shown by a yellow star in (a). (c) An example of a non-VLFE signal which was discarded by the beamforming analysis described in Section 2.3. The direction of this signal is shown by a blue arrow in (a). To enhance VLFE signals at available stations, amplitudes of noisy stations (PUCA, TENO, IRZU, HDC5, F4) are set as zero.

13

(a) 2005/08/10 03:53:47, 85.8ºW 9.4ºN

Correlation coefficients

log $_{10}$ (Moment rate [Nm/s]) Only CC > 0.9 x the maximum CC

(b) 2005/08/17 23:32:37, 85.7ºW, 9.3ºN

Correlation coefficients

$\log_{10}$ (Moment rate [Nm/s]) Only CC > 0.9 x the maximum CC
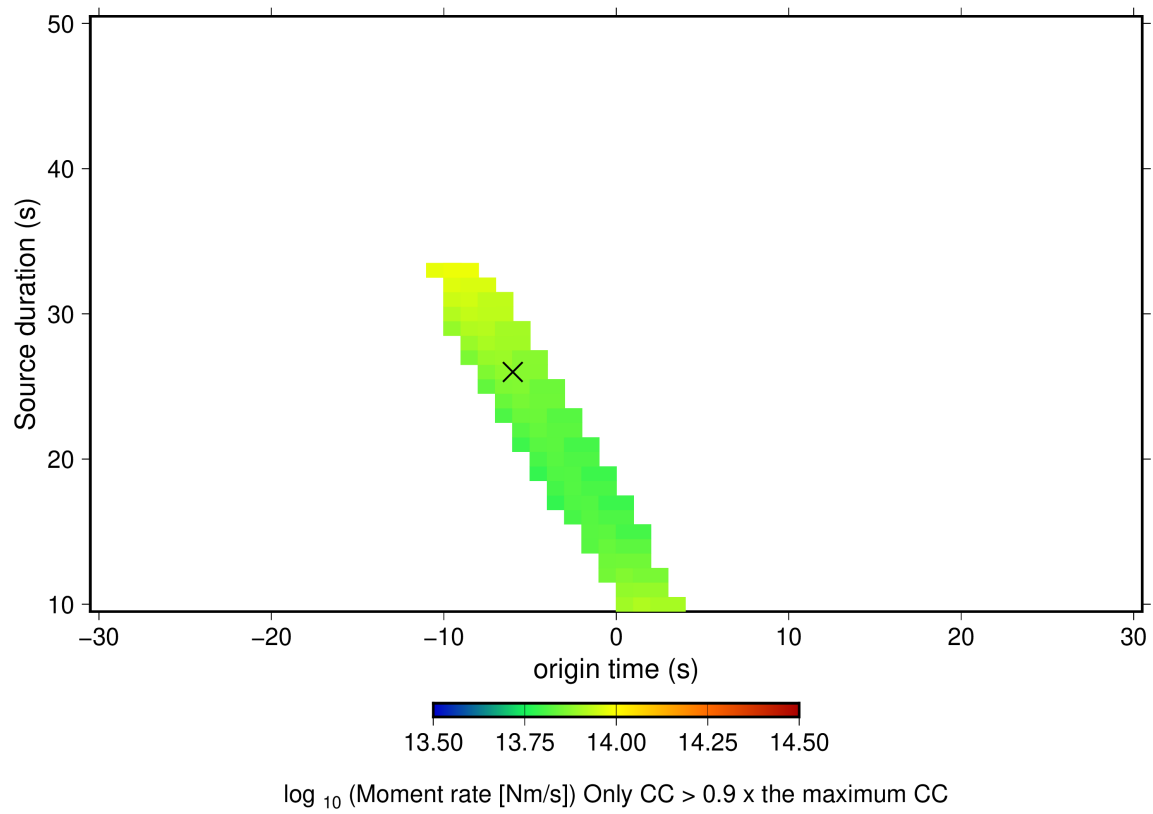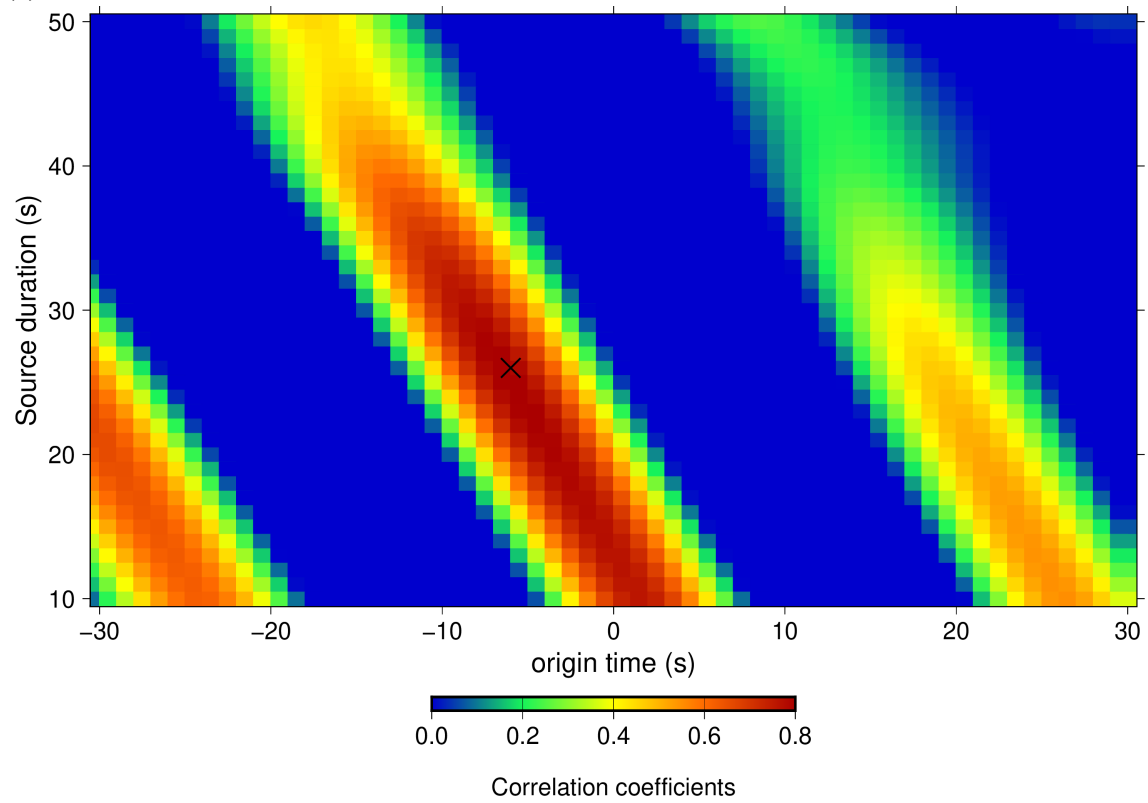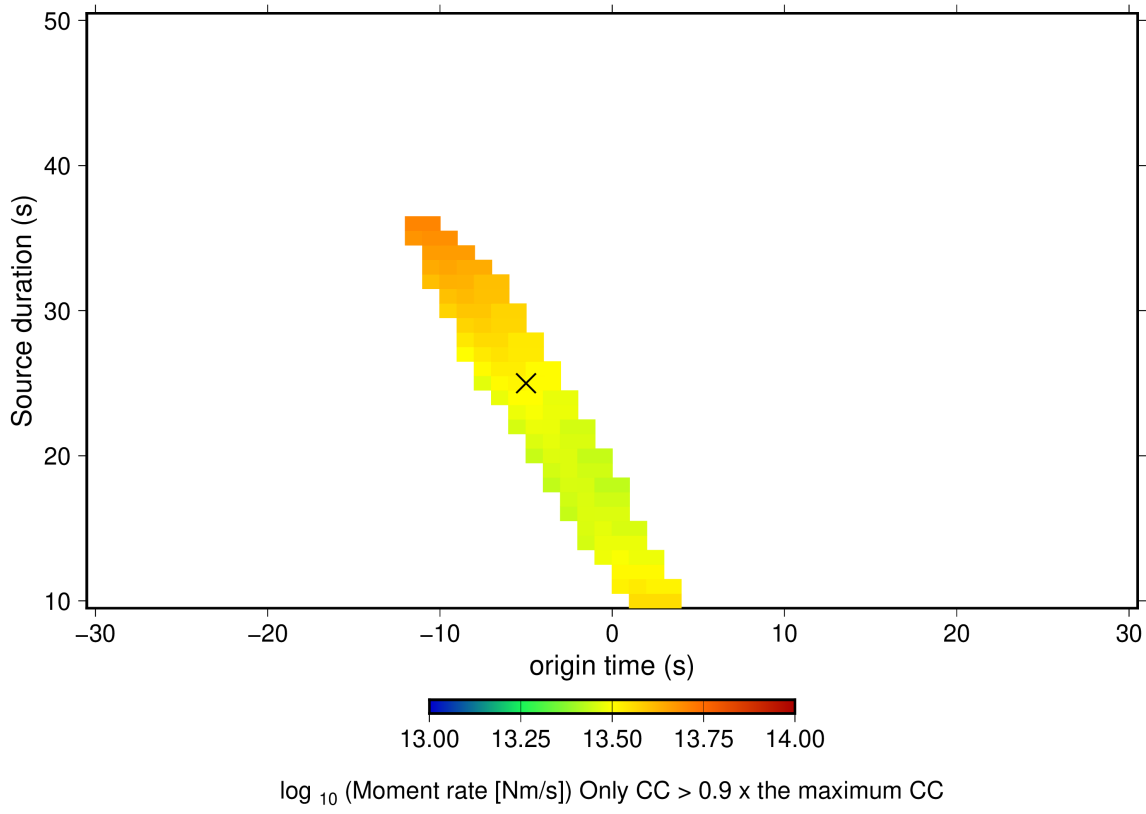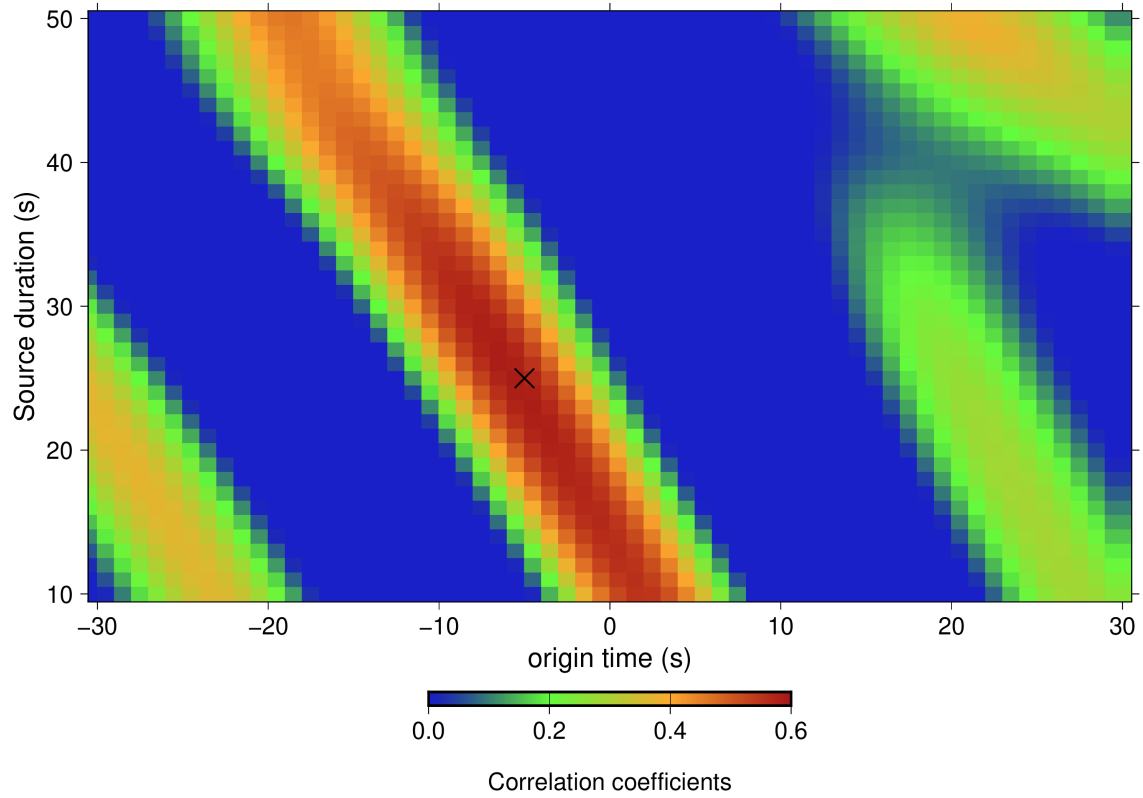
Figure S6. Distributions of CCs and moment rates when origin time and source duration changed. The cross shape indicates the combination of the origin time and the source duration when the CC is the highest.

(a) 2005/12/10 19:45:42 Mw 4.0 Depth: 42 km

(b) 2005/10/06 15:48:14 Mw 3.8 Depth: 29 km
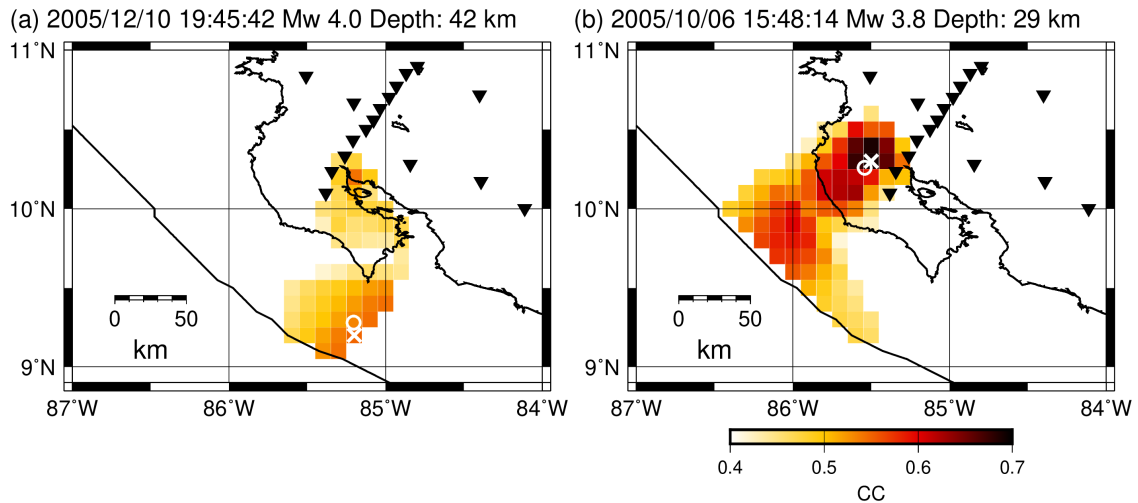
Figure S7. CC distributions between synthetic and observed waveforms of regular earthquakes in the (a) updip and (b) downdip events. Circles and cross marks in the maps are epicenters by the earthquake catalog constructed by El Observatorio Vulcanológico y Sismológico de Costa Rica and located by the method of this study, respectively. Black line and dashed contours in maps are the same as in Figure 1. Black inverted triangles in the maps are same as in Figure 6.

(a)

2005–08–10 03:00~ Vertical

0.02–0.05 Hz along dip
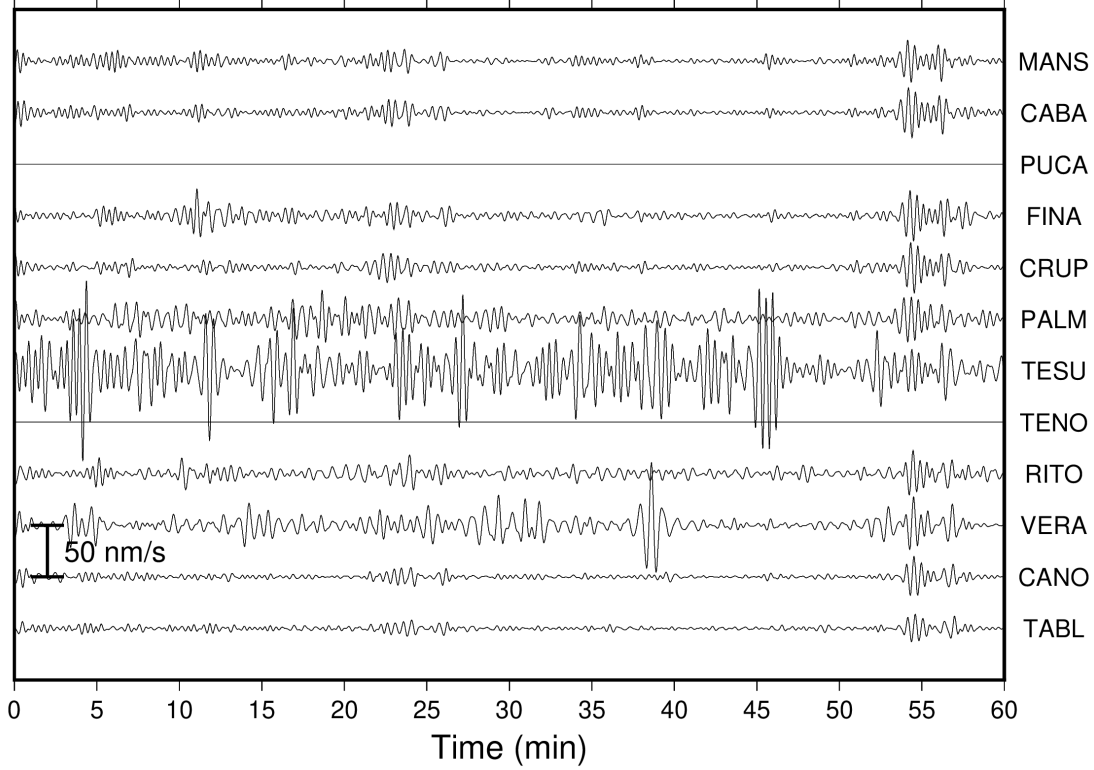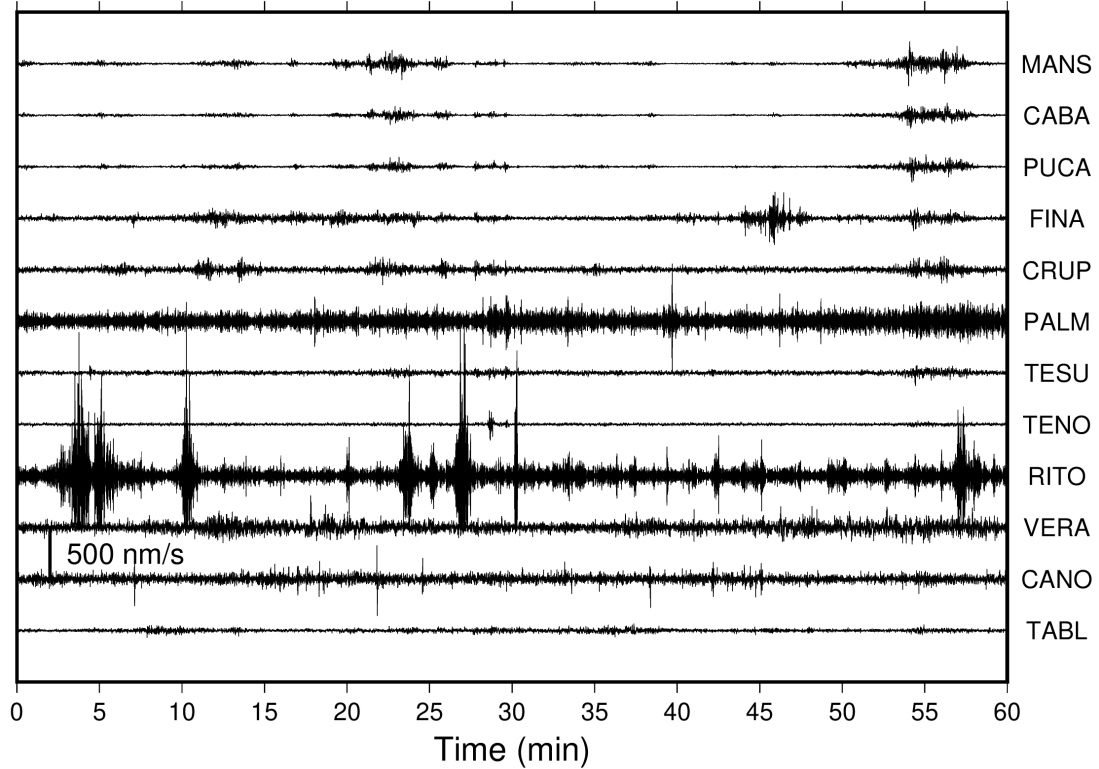
2–8 Hz along dip

(b)
2005–08–11 03:00~ Vertical

0.02–0.05 Hz along dip
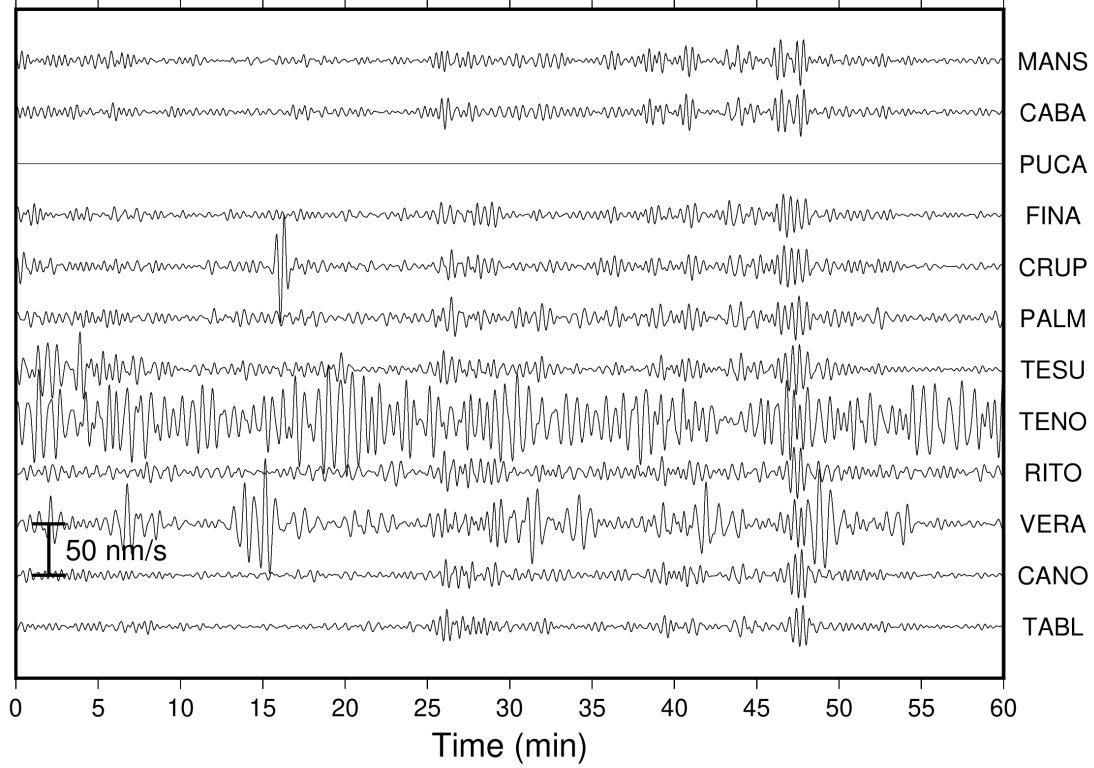
2–8 Hz along dip
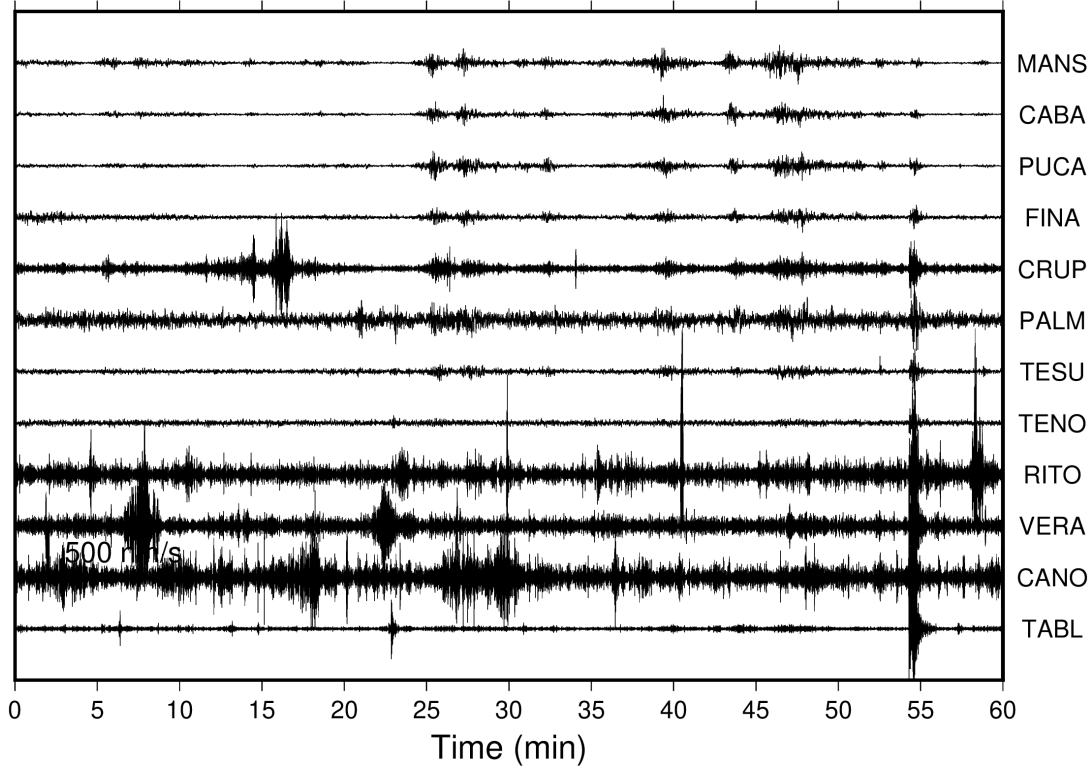
Figure S8. Example of waveforms when VLFEs in the frequency range of 0.02-0.05 Hz and tremors in the frequency range of 2–8 Hz occur simultaneously. Amplitudes of noisy stations are set as zero.


Elapsed time from maximum amplitude of observed waveform at MANS (sec)
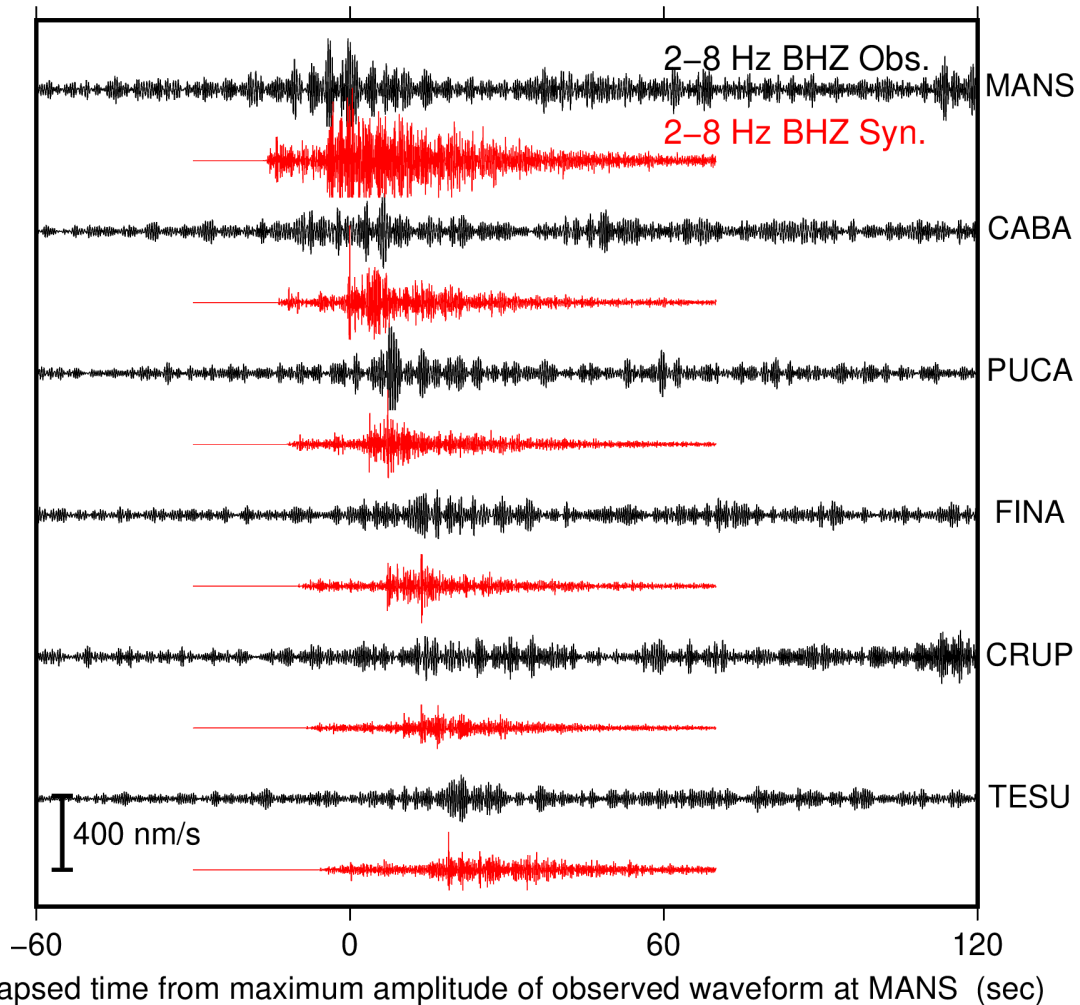
Figure S9. Example of observed (black) and simulated (red) waveforms of a tremor which corresponds to the VLFE located at 85.8°W and 9.4°N (origin time of the VLFE: 03:53:47, August 10, 2005 (UTC); the location is shown by a red beachball in Figure 2a) in the frequency range of 2–8 Hz. Seismograms are shown from 60 s before the time of the maximum amplitude of observed waveforms of the tremor at MANS. The assumed moment rate function was a Küpper wavelet with a source duration of 0.2 s.

19
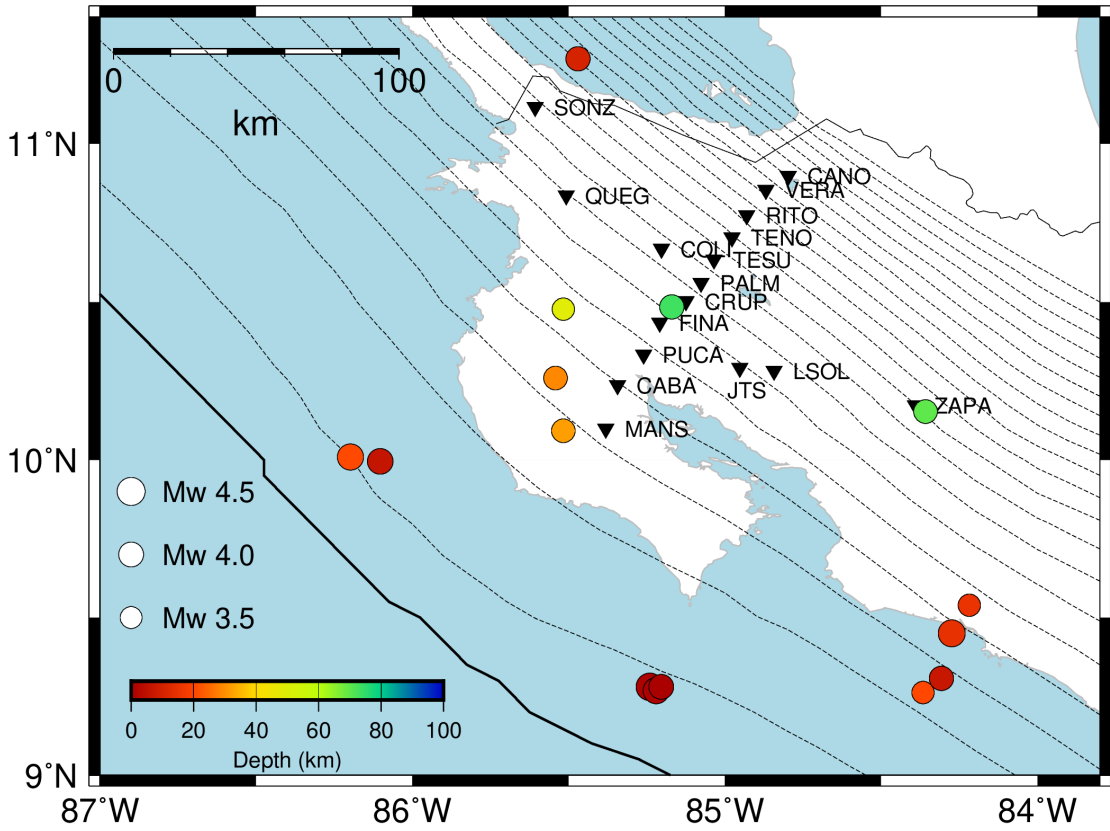
Figure S10. Distribution of earthquakes used in the estimation of the quality factor and site amplification factors. Inverted triangles, black line, and dashed contours are the same as in Figure 1.
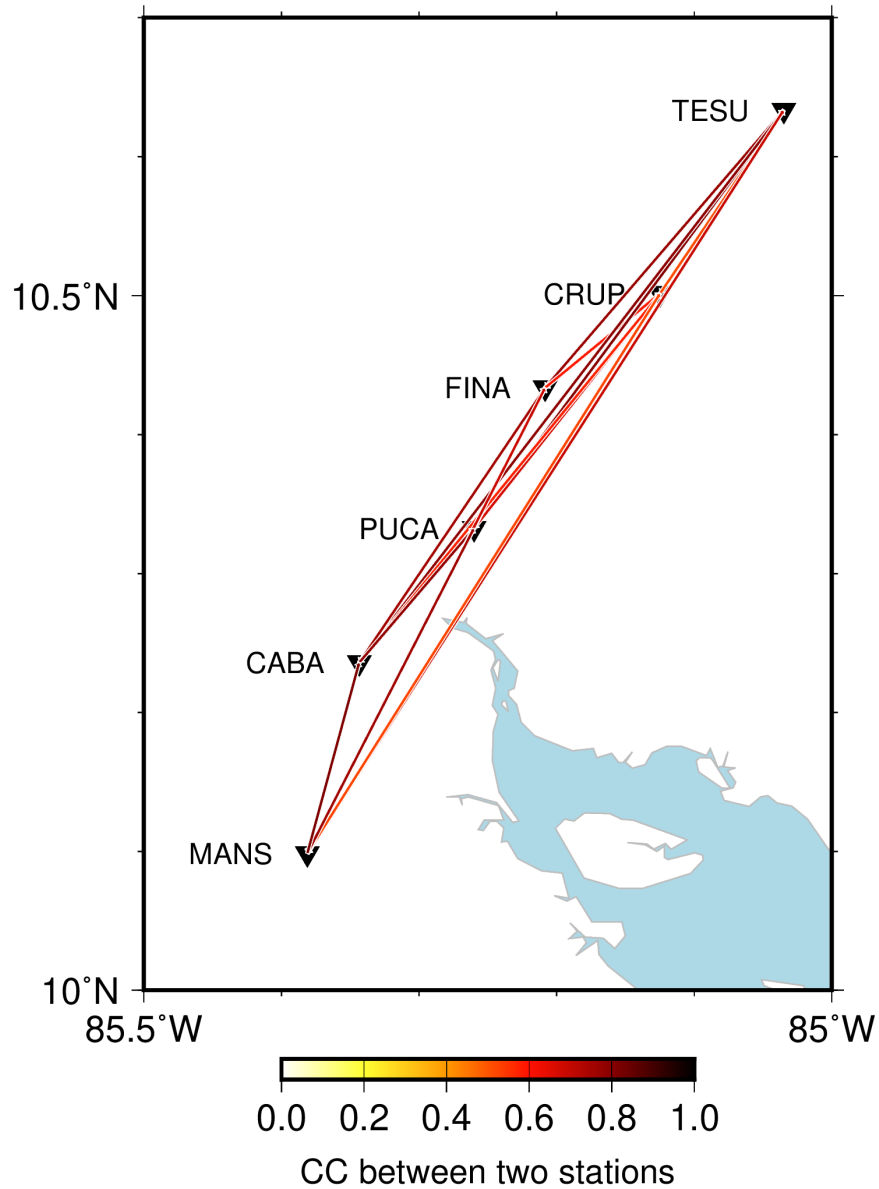
Figure S11. Distribution of CCs between envelope waveforms of station pairs for the event of Figure 3. The color of a line between two stations indicates the CC between the two stations. Epicenter of this event is shown by the red beachball in Figure 2. Inverted triangles are the same as Figure 1.

Table S1. Physical parameters of each layer in the velocity structure model used for computing template waveforms.

	V_p (km/s)	V_s (km/s)	ρ (kg/m³)	Q_p	Q_s
Air	0.0	0.0	1	10^{10}	10^{10}
Sea water	1.5	0.0	1,040	10^6	10^6
Upper sediments	2.2	0.8	2,000	260	150
Middle sediments	3.9	2.1	2,400	680	400
Lower sediments	5.1	2.9	2,600	680	400
Upper crust	5.5	3.1	2,600	680	400
Middle crust	6.5	3.7	2,800	680	400
Lower crust	7.0	4.0	3,000	680	400
Oceanic crust layer 2	5.0	2.9	2,500	340	200
Oceanic crust layer 3	6.7	3.9	2,800	510	300
Mantle	8.1	4.7	3,200	850	500

Data Set S1. List of detected VLFEs. First column: year, second column: month, third column: day, forth column: hour, fifth column: minute, sixth column: second, seventh column: longitude, eighth column: latitude, ninth column: depth (km), and tenth column: magnitude, eleventh column: duration (s). Times are described in UTC.

Data Set S2. List of energy rates of tremors accompanied by VLFEs. First column: year, second column: month, third column: day, forth column: hour, fifth column: minute, sixth column: second, seventh column: longitude, eighth column: latitude, ninth column: depth (km), and tenth column: energy rate (J/s). Times are described in UTC.